RESEARCH ARTICLE

Novel dimensionless index for physically based assessment of thermal refugia characterizes off-channel habitat on gravel bed river

Carolyn E. Gombert[1] | Stephen T. Lancaster[2] | Gordon E. Grant[3] | Rebecca L. Flitcroft[3]

[1]Sedimentation and River Hydraulics Group, Bureau of Reclamation, Denver, Colorado, USA

[2]College of Earth, Ocean, and Atmospheric Sciences, Oregon State University, Corvallis, Oregon, USA

[3]Pacific Northwest Research Station, U.S. Forest Service, Oregon, USA

Correspondence
Carolyn E. Gombert, Sedimentation and River Hydraulics Group, Bureau of Reclamation, Denver, CO, USA.
Email: cgombert@usbr.gov

Abstract

In the Willamette River, OR, main channel temperatures can be too warm for cold water fishes, causing fish to concentrate in secondary channel features that provide thermal refugia. However, temperature regimes vary among and within features. Improved understanding of physical processes controlling thermal regimes is needed. This study developed a dimensionless index for assessment of thermal refugia on the upper Willamette River. The novel hyporheic insolation (HIN) index uses minimal field measurements to predict thermal refugia resulting from buffering. Continuous water temperature measurements at one side channel, eight alcoves, and six beaver ponds provided data to ground truth calculated $\mathbb{H}_{in}$ predictions. Water temperature records were first used to characterize stratification at sites. Calculation of the Richardson number, an index of stability, showed two well-mixed sites and 13 stratified sites. At stratified sites, calculated $\mathbb{H}_{in}$ values characterized the ratio of cooling flux from hyporheic discharge to heat flux from incoming solar radiation. As $\mathbb{H}_{in}$ increased, measured temperatures at sites decreased. Despite overall scatter, a logarithmic fit to bin-averaged $\mathbb{H}_{in}$ values showed $R^2 = 0.91$. Calculations suggest that secondary channel features characterized by stratification and cool hyporheic discharge can provide thermal refugia. Accordingly, the HIN index may serve as a practical tool grounded in physical processes governing temperature across a floodplain.

KEYWORDS
temperature, hyporheic zone, fish, geomorphology, fluvial processes, surface water hydrology

1 | INTRODUCTION

Cold water anadromous fish species shelter in pockets of cool water known as thermal refugia to avoid heat stress (Ebersole et al., 2001; Sedell et al., 1990; Torgersen et al., 1999). Main channel temperatures have continued to warm as the climate changes (Dugdale et al., 2018; Fullerton et al., 2018; van Vliet et al., 2013). In addition, human population growth will increase demands on water resources and floodplains as the century progresses (Gleick, 2000). Identifying, preserving, and enhancing thermal refugia is imperative.

Stream temperature models can be useful tools for decision makers focused on providing thermal shelter to cold water fishes. Such models can offer a better understanding of water temperatures along a river corridor and can suggest the impacts associated with restoration or

wileyonlinelibrary.com/journal/jawr

Research Impact Statement

The novel hyporheic insolation (HIN) index predicts locations of thermal refugia along gravel bed rivers and advances our understanding of physical processes controlling water temperature in secondary channel features.

management decisions. One-dimensional (1D) models are able to estimate stream temperature on a watershed scale (Caissie, 2006). However, 1D models of mainstem temperatures do not sufficiently capture thermal heterogeneity at the micro-habitat level (Dugdale et al., 2017). Similarly, two-dimensional (2D) and three-dimensional (3D) temperature models, while able to represent hydrologic and hydraulic processes in greater detail, are limited by the quality and resolution of input data (Cole & Wells, 2006). Robust tools for predicting locations and quantities of cold water habitat are still needed.

Descriptive models of stream temperature leverage field measurements to categorize thermal heterogeneity at various scales. At the reach scale, high-resolution distributed temperature sensing and thermal infrared measurements can augment process-based modeling to estimate the spatial distribution of cold water fish species (Dzara et al., 2019). Nonetheless, the instrumentation and resources required for such work preclude its application to an entire river. At the catchment scale, remotely sensed temperature metrics have been used to classify four distinct thermal regimes tied to events related to salmon life histories (Shaftel et al., 2020). While Shaftel and colleagues were able to identify climate and landscape drivers shaping thermal regimes in the Matanuska-Susitna Basin, they do not specifically address the river-floodplain system. The development of tools to estimate the location and proportion of available cool water habitats on a scale relevant to river management remains incomplete.

Advancement of tools able to predict the distribution and quality of thermal refugia has been hindered by the fact that physical processes controlling river temperature heterogeneity remain difficult to isolate (Hannah & Garner, 2015). Most work on heat transfer processes in rivers has focused on heat fluxes in the main channel (Figure 1). Yet on complex river-floodplain systems, such as the Tagliamento River in Italy, spatial variation in water temperature along the mainstem is small compared to thermal heterogeneity observed across the floodplain (Arscott et al., 2001; Tonolla et al., 2010). In smaller streams, narrow channel widths and forested canopies can prevent incoming solar radiation from significantly increasing water temperature (e.g., Beschta & Taylor, 1988; Johnson, 2004; Johnson & Jones, 2000). In larger rivers, greater channel widths are unlikely to be in full shade, particularly during midday, and the influence of riparian shading on water temperature is smaller (Jackson et al., 2021; Poole & Berman, 2001). Furthermore, given water's large heat capacity and a main channel's large volumetric flow rate, inputs from the subsurface may only alter the water temperature of the well-mixed mainstem by a fraction of a °C (Burkholder et al., 2008). However, heat transfer mechanisms controlling temperatures observed in secondary channel features are not as well understood as the drivers controlling mainstem temperatures.

Secondary channel features include side channels, which are connected to the main channel at both their upstream and downstream ends, and alcoves, which are connected to the mainstem generally at the downstream end. While side channels and alcoves can serve as thermal refugia for cold water fishes (Stevens & DuPont, 2011; Wallick et al., 2013), differentiation between thermal regimes of different secondary channel features within the same reach is lacking. Thermal heterogeneity across side channels and alcoves results from heat transfer process operating at a different scale than the processes controlling temperatures in the mainstem (Figure 1a). For example, inputs from the subsurface may play a more significant role in secondary channel features. Subsurface discharge includes both groundwater and hyporheic water. Groundwater consists of precipitation that has infiltrated into the subsurface and comes to rest in the saturated zone below the water table. While groundwater discharge that enters a river channel originates from a neighboring aquifer, hyporheic water is sourced more locally. Specifically, hyporheic flow is river water that enters sub-aqueous streambed sediments beneath or near the channel (i.e., the hyporheic zone), flows down-gradient, and reemerges into the river or off-channel water bodies. If hyporheic water travels along flowpaths of sufficient lengths, it is possible for dispersion in the subsurface to attenuate temperature oscillations that are present when the river water enters the hyporheic zone. When compared to main channel temperature cycles, hyporheic zone cycles can be buffered (i.e., a difference in range) or lagged (i.e., a difference in phase) on either a diel or an annual period, as determined by hyporheic flowpath length, hydraulic gradient, and hydraulic conductivity (Arrigoni et al., 2008; Burkholder et al., 2008). A shorter flowpath, for example, may have a hyporheic temperature cycle lagged by 12 h, discharging water that, relative to the main channel, is cooler during the day but warmer at night. Longer subsurface flowpaths, however, may operate on an annual period corresponding to greater attenuation. In the summer, hyporheic flow reemerging will be consistently cooler than water in the main channel. Yet in the winter, it will be consistently warmer. Discharge of hyporheic water cooler than the mainstem may be one of the heat transfer mechanisms shaping the temperature variations that provide thermal refugia to cold water fishes.

The Willamette River is a representative gravel-bed river-floodplain system in Oregon, USA, a region where cold water species like trout and salmon are temperature limited. The upper Willamette River provides important rearing habitat for juvenile spring Chinook salmon, as
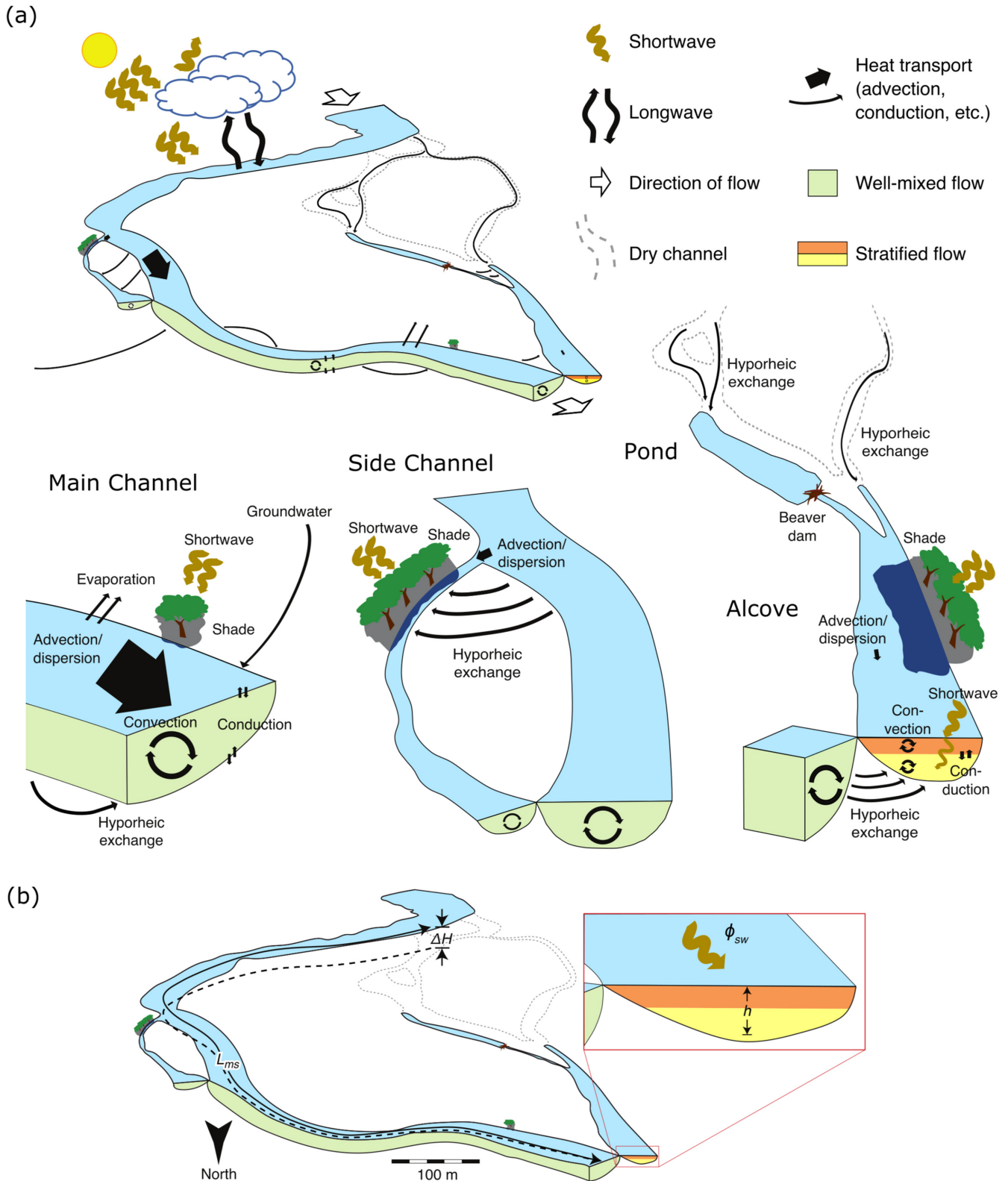
FIGURE 1 Schematic diagram, based on an oblique aerial photograph of the Willamette River, Oregon, of the heat budget (a) and key variables in dimensional analysis (b). (a) In water bodies with large enough flow velocities, advection and dispersion dominate local heat transport and, with convective mixing, make water temperature nearly uniform; bare-gravel surfaces are abundant, and channel banks may have sparse riparian vegetation, which shades relatively little of wide channels. In ponds and alcoves cut off from surface flow, stratification into shallow and deep layers prevents mixing, and results in attenuation of shortwave radiation to deep layers, where hyporheic or groundwater inputs may dominate temperature. (b) Key variables in dimensional analysis include shortwave radiation, ϕ_{sw}, mainstem length, L_{ms}, and change in head along the hydraulic flowpath, ΔH.

well as serving as a corridor for out-migrating smolts that are leaving freshwater to rear in estuary and marine environments (Schroeder et al., 2016). Thus, the Willamette must be able to provide habitat below critical temperature limits coincident with the adult spawning migration, as well as for the rearing and outmigration of juveniles.

Adequate levels of dissolved oxygen (DO) are also an important habitat quality for fishes. For salmonids, DO levels may partially restrict suitable cold water habitats (Ebersole et al., 2003). Accordingly, Oregon Department of Environmental Quality regulations for DO in "water bodies … providing cold-water aquatic life," which include the Willamette River Basin, outline "6.0 mg/L as an absolute minimum" (ODEQ, 2007). DO levels in the Willamette vary throughout the diel cycle on both the mainstem and in secondary channel features (Smith et al., 2020). Continuous DO data captured by Smith and colleagues in the upper Willamette suggest that, depending on river stage, secondary channel features either track main channel DO levels at high stage or exhibit a greater range at low stage. While this study focuses primarily on a physically based framework that describes the heat-related characteristics of secondary channel features, it also considers biologically based metrics such as DO, making an effort to keep the complex nature of riverine processes in view.

In an effort to elucidate the physical processes driving observed thermal heterogeneity observed in rivers and to address the need for predictive models at the river-floodplain scale, this study seeks to: (1) quantify thermal variability in and across secondary channel features, (2) use those data to ground-truth a new physically based dimensionless index for assessment of thermal refugia resulting from thermal buffering along long hyporheic flowpaths, and (3) identify some of the dominant physical processes controlling water temperature in secondary channel features. We seek to explore how field measurements can be put into a physically based framework rather than into a model to identify key drivers of water temperatures in secondary channel features. The success of this endeavor will be measured by the degree to which our framework can plausibly explain variations in water temperature and, by doing so, help establish reasonable expectations for identification and preservation of thermal refugia in gravel-bed rivers.

2 | STUDY SITE

Data collection took place on the upper Willamette River, a large, gravel-bed river in northwestern Oregon, USA (Figure 2a). The Willamette River is representative of gravel-bed rivers across the Pacific Northwest that provide key habitat for cold water fish species, many of which are listed as threatened. The upper Willamette offered a study site ideal for collection of water temperature data both in the main channel and in secondary channel features.

The Willamette flows from south to north through a wide, structural valley bounded on the east by the Cascade Range and on the west by the Oregon Coast Range. Our study area comprised two reaches of the upper Willamette River. The Harrisburg reach, located upstream of USGS gage 14166000 at Harrisburg (river km 199.5), has a contributing area of 8860 km^2. The Corvallis reach, located upstream of USGS gage 14171600 at Corvallis (river km 165.7), has a contributing area of 11,400 km^2. The average stream gradient of 0.98 m/km along the Harrisburg reach is steeper than the gradient of 0.62 m/km along the Corvallis reach (Dykaar & Wigington, 2000). A mean annual flow of 330 m^3/s (11,600 ft^3/s) occurs at the Harrisburg gage while a mean annual flow of 370 m^3/s (13,100 ft^3/s) occurs at the Corvallis gage.

The banks of the upper Willamette are predominately comprised of erodible Holocene alluvium which is set atop older Pleistocene deposits. The Pleistocene units consist of partially cemented gravel and a top set of weathered silt, which is itself overlaid with rhythmically bedded Missoula flood deposits composed of both weathered silt and clay (O'Connor, 2001). The partially cemented Pleistocene terrace is 2 to 5 times more resistant to bank erosion than the Holocene alluvium (Wallick et al., 2006).

Within the erodible Holocene alluvium floodplain, the upper Willamette is dynamic and typically has multiple threads along a significant fraction of its length, especially in the reaches with unreinforced banks on both sides of the river (<25%; Wallick et al., 2007). The U.S. Army Corps of Engineers operates eight flood-control dams upstream of Harrisburg, nine upstream of Corvallis. At the USGS 14174000 gage at Albany (the nearest with a long enough record), the mean annual flood discharge was 3240 m^3/s prior to flood control (WY 1893–1941) and 1840 m^3/s after (WY 1973–2019); mean annual flood stage dropped by 2.0 m. In the present regime of flood control, high flows still lead to changes in the channel planform, although those changes are less frequent and dramatic than before flood control. The dynamic quality of the upper Willamette River continues to allow for the creation of new secondary channel features such as the alcoves, side channels, and ponds instrumented in this study.

The climate of the upper Willamette Valley is characterized by cool, wet winters, and dry, warm summers. Average annual precipitation in the upper Willamette Valley is 162 cm (USGS StreamStats) and falls predominantly as rain during the period from October through June. Summer flow in the upper Willamette is predominantly from springs in the Cascade Range and from reservoirs, which are managed in the summer to increase discharge and thereby mitigate high stream temperatures. Daily maximum stream temperatures at the Harrisburg gage typically exceed the regulatory standard of 18°C from mid-July to mid-August, and even daily minimum temperatures exceed the standard for much of that time (ODEQ, 2007).
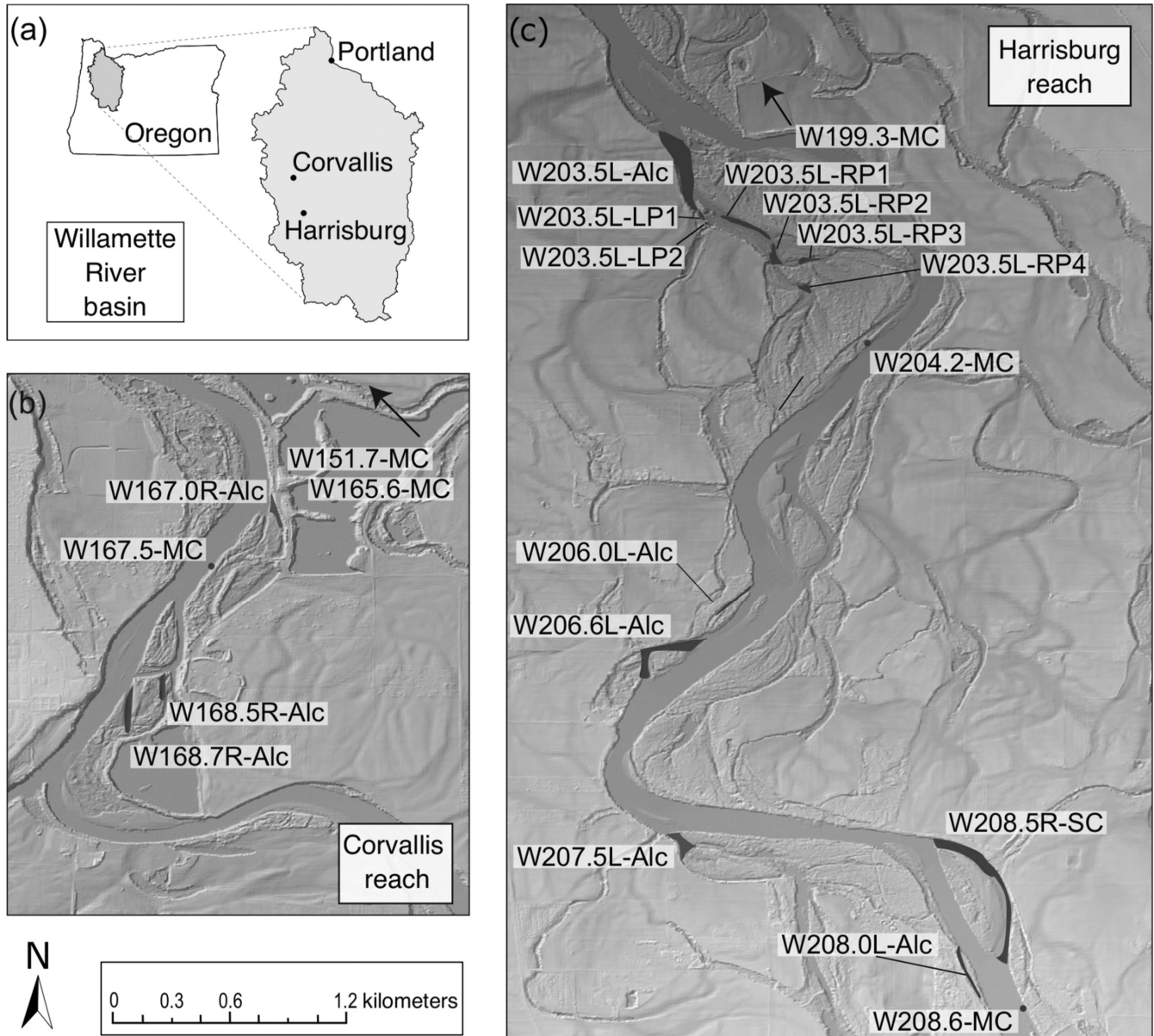
FIGURE 2 The study area is located in the Willamette River basin (a) and comprises the Corvallis (b) and Harrisburg (c) reaches. Off-channel sites, including eight alcoves, six ponds, and one side channel, are masked in dark gray; mainstem site locations are indicated with dark gray circles; all sites are labeled; the map is a National Elevation Dataset 10 m Digital Elevation Model paired with a hillshade background. Downstream locations of Harrisburg (c), Corvallis (b), and Albany gages (b) are indicated with arrows and labels using Willamette River Slices framework, bank location, and feature type.

3 | METHODS

3.1 | Field measurements

The goal of measurements and observations in the field was to characterize thermal regimes in secondary channel features, including side channels, alcoves, and beaver ponds, within the area defined by the modern floodplain of the upper Willamette River. Concurrent measurements in both secondary channel features and the main channel allowed for characterization of temperatures in the secondary channel features relative to temperatures in the main channel. We also recorded point measurements of DO at most secondary channel features.

3.1.1 | Measurement locations

Aerial photographs from May 2016 facilitated the identification of off-channel sites grouped within two study reaches along the upper Willamette River: Corvallis (Figure 2b) and Harrisburg (Figure 2c). The selected reaches were accessible by boat and contained a diversity of secondary channel features, including side channels, alcoves, and beaver ponds. In general, we define side channels in the study as being connected, with no discontinuity, to the main channel at both their heads, where flow is diverted from the main channel, and at their mouths, where flow rejoins the main channel. Alcoves, on the other hand, are off-channel water bodies with only one connection to the main stem, almost always at the downstream end. Along the upper Willamette, some alcoves occur on a former channel path that also includes ponds, or stretches of deep, flat water. Specifically, ponds are marked at their downstream mouths by a beaver dam and at their upstream heads with either another beaver dam or a connection to dry land (Figure 1a).

In total, 15 secondary channel features were instrumented. These off-channel sites included one side channel, eight alcoves, and six beaver ponds. Twelve of the off-channel sites, including the side channel and all of the beaver ponds, were located in the Harrisburg reach. The remaining three alcoves were located downstream in the Corvallis reach. In addition, instruments were deployed at three locations along the main channel. Two of the main channel deployments were located in the Harrisburg reach (Figure 2c). One was located in the Corvallis reach (Figure 2b).

We adopted a naming convention in which sites were identified by feature type, bank location, and a river kilometer based on the Willamette River Slices ("W") Framework (Hulse et al., 2002). Feature types included a side channel ("SC"), connected to the mainstem at both the upstream head and downstream mouth; alcoves ("Alc"), connected to the mainstem only at the downstream mouth; ponds ("P"), where beaver dams impounded water within abandoned channels on the floodplain; and, lastly, the main channel ("MC"). Off-channel sites had either right-bank ("R") or left-bank ("L") locations identifying the bank from which the feature originated, where right and left were determined with respect to the downstream direction. River kilometer numbers were assigned based on location of the upstream head for side channels, the downstream mouth at the confluence with the main channel for alcoves, the mouth of the downstream alcove for ponds, or the instrument itself for the main channel.

At the off-channel sites, a rangefinder (Nikon) and hip chain were used to measure the length of each secondary feature from its upstream terminus to its downstream mouth or dam in the case of beaver ponds. Based on these longitudinal measurements, instrumented columns were placed at head, midpoint, and mouth locations, at 15 m (±5 m) downstream of the upstream terminus, equidistant between upstream terminus and mouth or dam, and 30 m (±10 m) upstream of the actual mouth at the confluence with the mainstem or the dam, respectively (Figure 3a). Columns were located along the centerline in side channels and alcoves and along the thalweg in ponds.

At each column, measurement stations were located at three elevations, that is, bottom, middle, and top (Figure 3b), relative to the total water depth. If the total water depth was shallower than 0.45 m, stations were located at only two elevations, bottom and top. At the one side channel site, one column with two stations was located at the midpoint of a section of shallow channel upstream of a riffle; in the deep water downstream of the riffle, three columns of three stations each were located, as in alcoves, at head, midpoint, and mouth (Table 1). Each mainstem site contained only a single station near one bank and at 0.15 m (±0.05 m) above the bed, with the logger secured by means of the buoy-weight (3 kg) method or by fastened atop of a cinder block (13.5 kg). Past laterally averaged water temperature models calibrated to Willamette River data show a single measurement location to be sufficient for capturing water temperature on the main stem in our study reach (Rounds & Stratton Garvin, 2022).

3.1.2 | Temperature measurements

From July through September 2017, Onset Hobo Tidbit v2 data loggers were deployed to measure and record water temperatures (±0.2°C) at 15-min intervals. In secondary channel features, the temperature loggers were secured at all measurement stations, for example, three columns of three stations each for a total of nine loggers at each off-channel site (Figure 3). At each of the 15 off-channel sites, the average deployment period for measurement stations was 11 days, but varied from 2 to 37 days, where only days with instruments deployed from midnight to midnight are counted (Table 1). The duration of the period of deployment of loggers at a given site was effectively arbitrary. Our characterization of the physics governing water temperature across the river-floodplain system required collection of the greatest number of measurements under the widest range of site conditions. At the three mainstem sites, loggers were deployed for the entire duration of the study. Extended deployment times for mainstem loggers ensured that comparison between water temperatures in secondary channel features and in the mainstem was always possible and that repeated deployment of main channel sites was not required.

3.1.3 | Flow measurements

We used a flow meter and salt dilution to measure discharge and flow velocity at five sites (Table 1). Each of these five sites exhibited shallow surface flow with flow velocities great enough (≥0.15 m/s) to allow discharge measurement with a portable flow meter (Marsh-McBirney

NOVEL DIMENSIONLESS INDEX FOR PHYSICALLY BASED ASSESSMENT OF
THERMAL REFUGIA CHARACTERIZES OFF-CHANNEL HABITAT ON GRAVEL BED RIVER

| 621
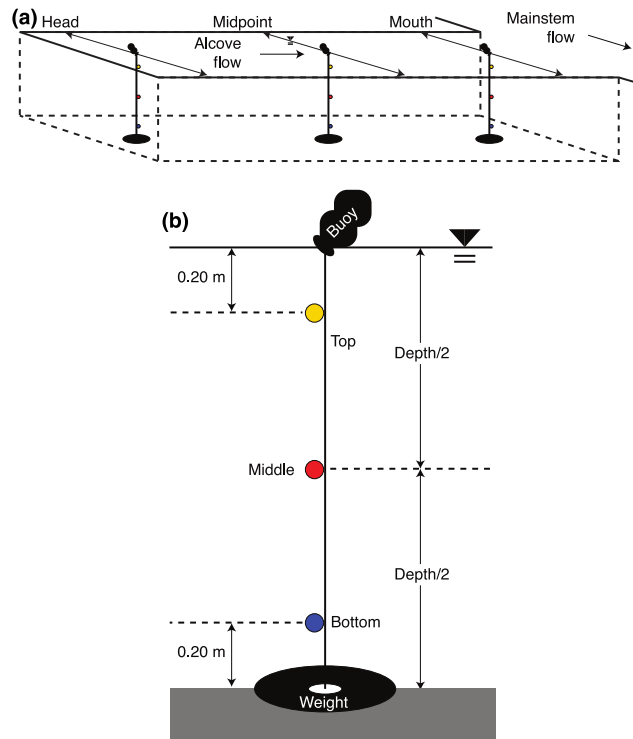
FIGURE 3 Temperature logger deployment scheme for off-channel sites: (a) longitudinal positions of vertical columns at the head, midpoint, and mouth of secondary channel features, and (b) vertical positions of loggers at three stations, bottom, middle, and top, along a cord suspended from a buoy and held in place by a weight (3 kg). Arrows indicate direction of flow in the main channel and in the alcove channel/alcove/pond.

FlowMate 2000; Hach Company) and a top-setting wading rod. At sites with slower velocities (e.g., ≤0.15 m/s), salt dilution was used to measure discharge (Table 1).

Prior to the salt injection, Onset HOBO U-24 conductivity-temperature (CT) loggers (±2 μS/cm) were calibrated with a known mass of salt and water from the alcove and then secured at middle and bottom stations of columns downstream of the salt injection location. Loggers were set to record measurements at 10 s intervals. At W206.6L-Alc, CT loggers were secured at the middle stations of the three centerline columns. At the head and midpoint locations, four more CT loggers were secured at middle stations on additional columns placed on both sides of the existing centerline columns, halfway to either bank. Each salt injection used a known mass of salt (Morton Pickling Salt) dissolved in water from the alcove and then spread across the width of the alcove at its upstream end. Time of injection and distance to CT logger stations were recorded. Flow velocities were then estimated from the timing of conductivity logger breakthrough curves and known logger distances from the salt injection location.

3.1.4 | DO measurements

DO point measurements were taken at 13 of 15 off-channel sites (Table 1). Using a handheld YSI-ProODO probe (±0.1 mg/L, Yellow Springs, Ohio, USA), we measured temperature (°C) and DO (mg/L) at all stations at 13 sites (Table 1). DO readings were recorded from July 24 through August 24 (Table 1) between 9:00 and 15:00 PDT. Unlike the automatic temperature and conductivity measurements recorded by loggers at fixed positions, the DO measurements were recorded by manually lowering the probe to the appropriate water column depth and recording a reading from the digital meter once it had reached a stable value. Due to the range in time-of-day for DO point measurements, it is possible that productivity resulting from photosynthesis by algae and other aquatic plants may not have been captured at all sites.

3.2 | Dimensionless index formulation and calculation

Temperature measurements collected in our 15 secondary feature sites provided the necessary data to ground-truth a new physically based dimensionless index allowing assessment of thermal refugia. Specifically, the new dimensionless hyporheic insolation, or HIN, index builds

TABLE 1 Summary of secondary channel feature measurements.

Site	Dimensions Len. (m)	Avg. dep. (m)	Temperature measurements No. stns.	No. cols.	Stns. per col.	Days of year	Stn-days	Col-days	Site-days	DO meas. Days of year	No. stns.	Flow measurements Method	Days of year
W167.0R-Alc	162	0.62	9	3	3	189–190	18	6	2				
W167.5-MC			1			189–226	38						
W168.5R-Alc	92	1.1	9	3	3	220–226	63	21	7	217	9		
W168.7R-Alc	187	1.3	9	3	3	192–197, 217–226	144	48	16	216	9		
			8	3	2/3/3	189–191, 198–216	176	66	22				
W203.5L-Alc	450	1.3	9	3	3	194–202	81	27	9	223	15	SD	201
			15	5	3	203–239	555	185	37	236	15	MM	201, 236
W203.5L-LP1	25	0.60	6	2	3	230–239	60	20	10	236	6		
W203.5L-LP2	10	1.4	3	1	3	230–236	9	3	3	236	3		
			6	2	3	237–239							
			8	3	3/2/3	248–251	24	8	4				
W203.5L-RP1	340	1.1	9	3	3	230–239	90	30	10	236	9		
W203.5L-RP2	100	2.4	9	3	3	230–243	126	42	14	236	9		
W203.5L-RP3	90	0.76	9	3	3	230–239	90	30	10	236	9		
W203.5L-RP4	50	1.8	9	3	3	245–254	60	20	10				
W204.2-MC			1			194–254	58						
W206.0L-Alc	146	0.82	9	3	3	200–204	45	15	5	205a	9	MM	205
										205b	9		
W206.6L-Alc	247	1.6	9	3	3	223–227	45	15	5	222	9	SD, MM	222
W207.5L-Alc	70	1.8	9	3	3	208–213	54	18	6	207	9	SD, MM	213
										214	9		
W208.0L-Alc	100	0.52	9	3	3	200–205	54	18	6	206a	9		
										206b	9		
W208.5R-SC	790	0.72	11	4	2/3/3/3	203–220	198	72	18	223	11	MM	202, 221
W208.6-MC			1			203–251	58						
Totals							2198	668	201				

Note: Days of year = Calendar day: 181 = June 30; 212 = July 31; 243 = August 31. Flow measurement methods: MM = Marsh-McBirney Flowmate 2000 with top-setting wading rod; SD = salt dilution with calibrated Onset HOBO U-24 conductivity-temperature loggers. Low stage days = 189–212; high stage days = 216–254 (Stage increase from August 1 to 3 = 213–215).

Abbreviations: Avg. dep., average depth at columns; DO, dissolve oxygen; Len., feature length; No. cols., number of columns at site; No. stns., number of stations at site.

NOVEL DIMENSIONLESS INDEX FOR PHYSICALLY BASED ASSESSMENT OF
THERMAL REFUGIA CHARACTERIZES OFF-CHANNEL HABITAT ON GRAVEL BED RIVER

JAWRA
JOURNAL OF THE AMERICAN WATER RESOURCES ASSOCIATION

AMERICAN
WATER RESOURCES
ASSOCIATION

623

on heat transfer mechanisms observed in secondary channel features. Its formulation and calculation depend on three processes illustrated in Figure 1: (1) advection, or the transfer of heat downstream with the movement of water, (2) shortwave radiation from the sun, and (3) hyporheic exchange between surface water and hyporheic water and/or groundwater. Dimensional analysis for the HIN index is available in the Supporting Information. Application of the HIN index first involves determining presence of stratification, or dynamic stability. Then, if stratification is present at a site, the HIN index can be used to estimate the ratio between cooling from hyporheic discharge and heating from insolation. Calculations performed using field measurements and publicly available datasets are as follows.

3.2.1 | Stratification as referenced by the Richardson number

Thermal stratification in a water column occurs when lower density warm water sits above higher density cold water. Stratification can be quantified with the Richardson number, which is defined as the ratio between destruction of turbulent kinetic energy by buoyant forces to the production of turbulent kinetic energy by shear forces. Neglecting the small correction for the compressibility of water, the gradient Richardson number for layers is

$$\mathbb{R}i = -\frac{\frac{g}{\bar{\rho}}\frac{\Delta\rho(T)}{\Delta z}}{\left(\frac{\Delta u}{\Delta z}\right)^2},\tag{1}$$

where g is acceleration due to gravity (m/s^2); $\Delta\rho(T)$ is the difference in density of water (kg/m^3) between layers, calculated as a function of the water temperature, T (K), in each layer; Δz is the difference in height above the bed (m) between layers; Δu is the difference in time-averaged, downstream flow velocity (m/s) between layers; and $\bar{\rho}$ is the average density across layers (kg/m^3) (Peixoto & Oort, 1992). Flow is stratified for $\mathbb{R}i > 0.25$. Below this threshold, lower values of $\mathbb{R}i$ indicate higher degrees of turbulence and well-mixed water columns.

We calculated the Richardson number at sites where velocity measurements were obtained directly, using published values for density variation with temperature (Rumble, 2018). We leveraged temperature gradient as a proxy to assess stratification in all study sites because we did not obtain velocity measurements for all secondary channel features. Our proxy for the Richardson number, then, can be defined as,

$$\mathbb{R}i_p = \frac{\Delta T}{\Delta z}.\tag{2}$$

Our systematic deployment of loggers at each off-channel site facilitated estimation of the proxy of the Richardson number (2) for layers represented by measurements at the top and bottom stations of each column.

3.2.2 | Cooling versus heating as referenced by the HIN index

For a stratified side channel, alcove, or pond, the HIN index assesses the relative ratio of cooling by hyporheic inflow and heating by insolation. Dimensional analysis that produced the HIN dimensionless ratio used a physics-based framework to develop a new tool for assessment of thermal refugia along gravel-bed rivers (see Supporting Information). Of the 10 values required for calculation of the HIN index, only one, that is, water depth, was measured at our sites in the field. All other values were estimated from public data sets, literature values, and publicly available aerial photographs. This allowed temperature measurements collected in secondary channel features to ground-truth the novel HIN index.

The HIN index presents the ratio of cooling by hyporheic inflow to heating by insolation with a dimensionless ratio as

$$\frac{\phi_{hr}}{\phi_i} \sim \mathbb{H}_{in} \equiv \frac{\rho c_w T_a}{e^{-\zeta h}\phi_{sw}}\sqrt{\frac{KS_oL_{ms}}{t_a}},\tag{3}$$

where ϕ_{hr} is relative cooling from hyporheic discharge, ϕ_i is relative heating from incoming solar radiation, $\mathbb{H}_{in}$ is termed the HIN index, ρ is the difference in density of water (kg/m^3), c_w is the specific heat capacity of water (J/kgK), T_a is the annual mean temperature in the main channel (K), ζ is the attenuation coefficient of light in water (1/m); h is depth below the water surface (m), ϕ_{sw} is the mean daily incoming solar radiation per unit area (W/m^2), K is hydraulic conductivity (m/s), S_0 is the mainstem water surface gradient (m/m), L_{ms} is the mainstem length (m), and t_a is the annual period (s). The HIN index is intended to be calculated on a daily basis. Our formulation of the HIN index predicts the location of thermal refugia resulting from thermal buffering along long hyporheic flowpaths. It does not capture thermal refugia that may be created by thermal lagging associated with shorter flowpaths.

TABLE 2 Summary of values for $\mathbb{H}_{in}$ calculations.

Site	T_a (K)	Mean ϕ_{sw} (W/m^2)	ϕ_{sw} std dev. (W/m^2)	L_{ms} (m)	S_0	K (m/s)	ζ (m/m)
W167.0R-Alc	285.45	954	13	500	6.2×10^{-4}	5×10^{-2}	5
W168.5R-Alc	285.45	914	66	1650	6.2×10^{-4}	5×10^{-2}	2
W168.7R-Alc (low stage)	285.45	966	10	1500	6.2×10^{-4}	1×10^{-1}	1
W168.7R-Alc (high stage)	285.45	926	72	1500	6.2×10^{-4}	1×10^{-1}	1
W203.5L-Alc (low stage)	284.55	964	17	2900	9.8×10^{-4}	5×10^{-1}	1
W203.5L-Alc (high stage)	284.55	926	57	2900	9.8×10^{-4}	5×10^{-1}	1
W203.5L-LP1	284.55	921	70	1000	9.8×10^{-4}	1×10^{-1}	1
W203.5L-LP2	284.55	612	204	700	9.8×10^{-4}	1×10^{-1}	1
W203.5L-RP1	284.55	923	66	550	9.8×10^{-4}	5×10^{-1}	1
W203.5L-RP2	284.55	921	70	700	9.8×10^{-4}	5×10^{-1}	0.5
W203.5L-RP3	284.55	921	70	1675	9.8×10^{-4}	5×10^{-1}	0.5
W203.5L-RP4	284.55	739	165	1625	9.8×10^{-4}	5×10^{-2}	1
W206.0L-Alc	284.55	972	58	350	9.8×10^{-4}	5×10^{-2}	1
W207.5L-Alc	284.55	972	12	5800	9.8×10^{-4}	5×10^{-2}	1
W208.0L-Alc	284.55	968	48	300	9.8×10^{-4}	5×10^{-1}	1

Note: Tabulated values used to calculate the hyporheic insolation index. T_a is mean annual temperature, K; ϕ_{sw} is the mean and standard deviation value of incoming solar radiation, W/m^2; K is hydraulic conductivity, m/s; L_{ms} is mainstem length measured from the upstream divergence of the secondary flowpath to the downstream extent of the secondary feature, m; S_0 is the mainstem water surface gradient, m/m; ζ is the attenuation coefficient of light in water, m/m.

Larger values of the HIN index should correspond to greater effects of hyporheic cooling relative to heating by insolation. Because greater hyporheic cooling (i.e., maximum "buffering") is associated with longer residence times in the subsurface, we expect that dispersion will lead to hyporheic inflow temperatures approaching the annual mean stream temperature as subsurface residence times approach a period of 1 year.

Calculation of $\mathbb{H}_{in}$ at stratified sites in our two study reaches included three terms sourced from public data sets (Table 2): (1) the mean annual stream temperature, K (T_a), taken from the USGS Harrisburg gage for the Harrisburg Reach and the USGS Albany gage for the Corvallis reach; (2) the mean daily incoming solar radiation per unit area (ϕ_{sw}) calculated from values measured at the Oregon AgriMet Weather Station Corvallis location (crvo) on column-days corresponding to instrument deployment dates at each site (Table 1); and (3) the mainstem length measured from the upstream divergence of the secondary flowpath to the downstream extent of the secondary feature (L_{ms}) (Figure 1b) estimated using aerial photos on Google Earth. Literature values informed another three terms (Table 2): (1) reach-scale stream gradient (S_0) obtained from Dykaar and Wigington (2000), (2) hydraulic conductivity (K) estimated from slug tests on both the Corvallis reach and Harrisburg reach (Fernald et al., 2006), and (3) the attenuation coefficient (ζ) estimated based on field notes and data collected for lakes in Oregon exhibiting oligotrophic, mesotrophic, and eutrophic conditions (Dodds & Whiles, 2010). Three terms were treated as constants: (1) the density of water, (2) the specific heat capacity of water, and (3) the number of seconds in a year. The only term sourced from field measurements required for $\mathbb{H}_{in}$ calculations was depth below surface water (h).

4 | RESULTS

4.1 | Thermal regimes

Temperature measurements at all sites consist of more than 2000 station-days recorded at 15-min intervals (Table 1). From August 1 to 3, 2017, a reservoir drawdown increased river stage by 0.5 m at the USGS Harrisburg Gage, and the elevated stage persisted through August. The averaged discharge for the week prior to the drawdown (July 25 through 31, 2017) was 120 m^3/s (4300 ft^3/s) while the averaged discharge measurements for the week after the drawdown (August 4 through August 10, 2017) equaled 215 m^3/s (7600 ft^3/s). A complete record of river stage at the USGS Harrisburg gage during the study period is available in the Supporting Information. The change in discharge, and the concomitant increases in water level, allowed data collection at sites before and after the change to cover a wider range of relevant conditions for evaluation of our physically based framework.

Selected time series shown in Figure 4 illustrate thermal regimes worthy of later discussion. The remaining records are available in the Supporting Information. A diel cycle of temperature fluctuations is evident at all stations (Figure 4), but amplitude and phase of fluctuation varied among sites, columns at a site, and, notably, stations on a column.

NOVEL DIMENSIONLESS INDEX FOR PHYSICALLY BASED ASSESSMENT OF
THERMAL REFUGIA CHARACTERIZES OFF-CHANNEL HABITAT ON GRAVEL BED RIVER

AMERICAN
WATER RESOURCES
ASSOCIATION

JAWRA
JOURNAL OF THE AMERICAN WATER RESOURCES ASSOCIATION | 625
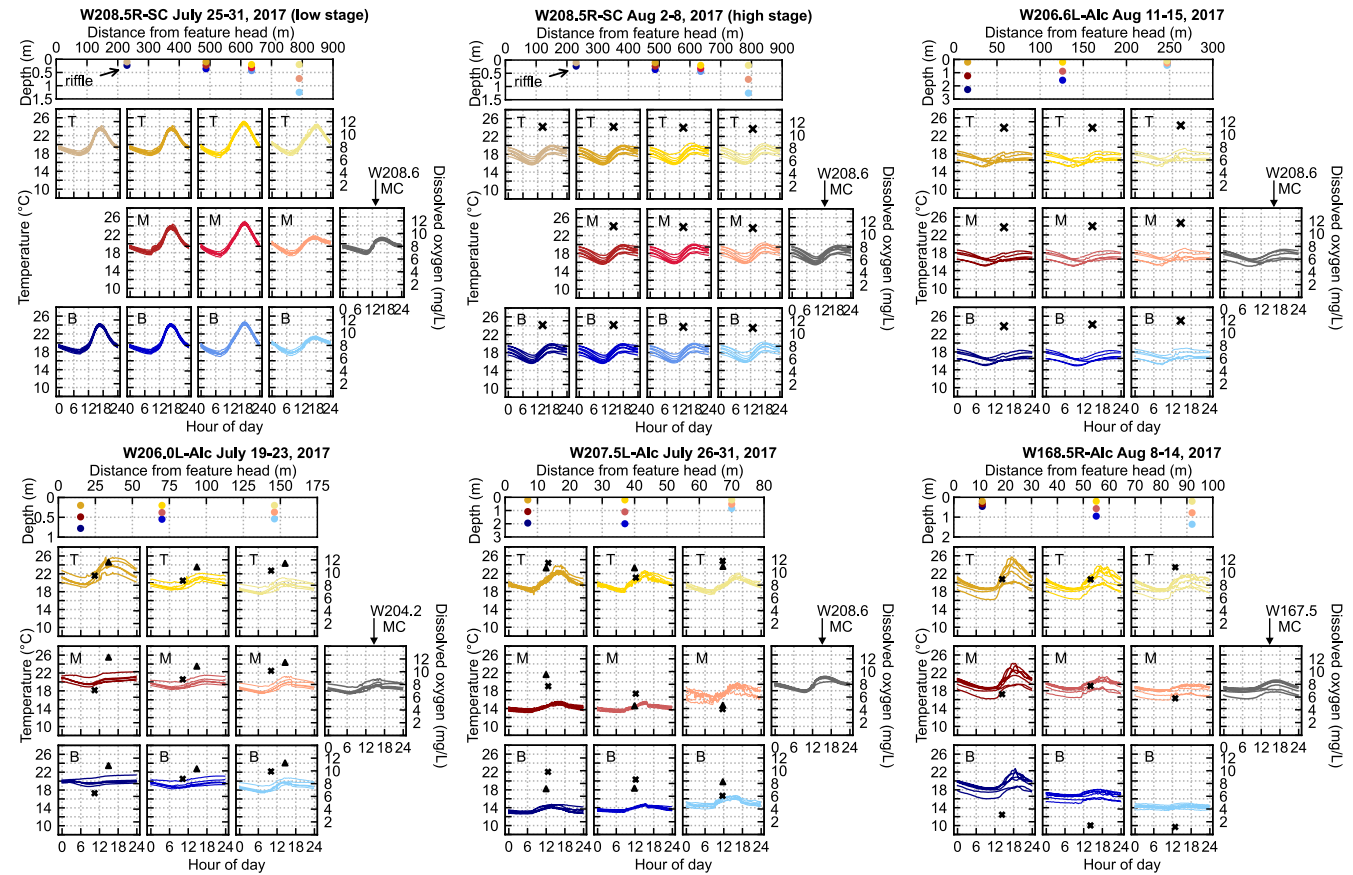
FIGURE 4 Water temperature (lines, left-hand *y*-axis) and dissolved oxygen (DO; "x" or triangle [if second point measurement completed, Table 1], right-hand *y*-axis) versus hour of day (*x*-axis), grouped by site and time period (site name and month/day of 2017 in group title), for up to 7 diel cycles each, for the side channel and four alcoves. All temperature and DO axes have the same scale on all graphs. In each grouping, each graph corresponds to one station at the site, plus one graph for the same days at the mainstem site indicated on the graph (B = bottom, M = middle, T = top; MC = main channel; Figures 2 and 3; Table 1). Depths of stations at each site are shown as well, plotted by distance from feature head. In total, 361 station-days at secondary channel features are shown.

Temperature variations with depth were consistent with stratification at 13 sites, including all six ponds and seven of the eight alcoves. (Alcove W206.6L-Alc did not present temperature variations with depth.) Water temperatures were always coolest near the bed and warmest near the water surface. Near-surface temperatures fluctuated with larger amplitude than near-bed temperatures. At 11 of the apparently stratified sites, water temperatures increased with increasing distance downstream, as at W207.5L-Alc (Figure 4). However, at two stratified sites, W206.0L-Alc and W168.5R-Alc, water temperatures at bottom, middle, and top stations all decreased with increasing distance downstream (Figure 4).

Water temperatures were nearly uniform with depth at two sites, W208.5R-SC and W206.6L-Alc (Figure 4). At both sites, near-bed temperature measurements were within 0.5°C of near-surface temperature measurements. Only one local exception was observed at the most downstream section of the deep side channel reach at low stage (Figure 4).

In the side channel and in the alcoves, daily minimum temperatures occurred in the morning between 08:00 and 09:00. Temperatures tended to peak in the late afternoon to early evening between 15:00 and 18:00. The time of daily maximum temperature varied with depth. For example, the peak temperatures recorded by the top and bottom loggers deployed at the head of W206.0L-Alc were offset by ~9 h (Figure 4). The time of daily maximum temperature also varied with distance downstream. That is, the daily maximum temperatures at the head, the midpoint, and mouth did not always occur at the same time of day.

Compared to secondary channel features, the amplitude of the diel temperature cycle in the main channel is small. Mainstem temperatures at higher stage were generally cooler than at lower stage. At lower river stage, loggers in the main channel reached their maximum between 15:00 and 16:00 in the Harrisburg reach, and between 17:00 and 18:00 in the Corvallis reach. At higher river stage, maximum temperatures at Harrisburg occurred between 19:00 and 20:00, while the maximum in Corvallis remained between 17:00 and 18:00.

In addition to temperature measurements presented here, we also consulted aerial photographs from different years to infer information about a site's geomorphic history. These images can indicate dates when a secondary channel feature may have been part of a former main

channel path, mark the date riparian vegetation began to emerge on a site, and suggest the upstream terminus of the feature's hyporheic flowpaths. Images from different years and at different stages are publicly available on platforms such as Google Earth. Using an aerial photo from June 28, 2017, we created a color-coded map of the thermal regimes throughout the two study reaches for features connected to the main channel at their mouths (Figure 5). All secondary channel temperatures illustrated represent the mean of the difference between bottom station and main channel temperatures recorded at the time when the top station of the column reached its daily maximum. For selected secondary channel features, images from other years, including 1994 and 2003 are also shown. Sites warmer than the main channel, such as W206.0L-Alc, do not have bottom-water temperatures deviate from main channel temperatures more than 2°C. W206.0L-Alc does not show historical evidence of development of sufficiently long relict channel paths that would allow for cool, buffered hyporheic discharge (Figure 5d). In contrast, colder sites, such as W207.5L-Alc remain connected at high stages to hyporheic flowpaths that extend for upwards of 5 km upstream (Figure 5c). Sites like W203.5L-Alc, for which temperature measurements may be found in the Supporting Information, were along the main channel path of the Willamette as recently as 1994. As a result, hyporheic discharge into W203.5L-Alc likely travels along a preferential hyporheic flowpath with high permeability and significant length, for example, 2.9 km (Figure 5b).

4.2 | DO in secondary channel features

DO levels were measured at 13 of the 15 study sites (the two sites with no measurements are W167.0R-Alc and W203.5L-PR4; instrument availability did not allow data collection at these sites possible). In general, DO point measurements varied by depth and by distance downstream (Figure 4). At two sites, W208.5R-SC and W206.6L-Alc, DO point measurements were between 10.3 and 11.9 mg/L, and differences between readings taken at different depths were small, that is, <0.1 mg/L. The most downstream section of W206.6L-Alc was an exception, with a slightly larger difference, that is, >0.5 mg/L, between the near-bed and near-surface readings at the mouth of the feature.

    At other alcoves, DO readings tended to show greater variation with depth, with differences upwards of 4 mg/L throughout the water column. Typically, levels of DO decreased with depth and increased with distance downstream. The lowest DO readings were taken at near-bed depths. The highest DO levels were recorded at the most downstream end of each feature at near-surface stations.

4.3 | Dimensionless numbers

4.3.1 | Richardson number describes stratification in secondary channel features

Values of Richardson number were calculated for sites where flow velocities were measured, including the side channel and four alcoves. For reference, further discussion of these calculations may be found in the Supporting Information. Richardson numbers for a given column-day were graphed with temperature gradient for the same column-day to assess the temperature gradient alone as a proxy indicator of stratification (Figure 6). That is, Richardson number effectively contains temperature gradient in that the density gradient is a function of the top and bottom temperature measurement of each column-day, but small temperature gradients can result in stratification for small-enough flow velocities. Indeed, the results show that temperature gradients in stratified and mixed column-days overlap in the range 0.5–3.5°C/m. In general, column-days in alcoves were stratified, and column-days in the side channel were mixed. The exceptions are as follows: first, all column-days in W206.6L-Alc were mixed, that is, had $\mathbb{R}i < 0.25$; and second, at low stage, that is, prior to the reservoir release beginning August 1, all column-days at the mouth of W208.5R-SC were stratified, that is, $\mathbb{R}i > 0.25$. All $\mathbb{R}i$ values were calculated (and are plotted) using the temperature gradient at the time of the daily maximum temperature at the top logger (Figure 6). At each site, the near-surface water temperature generally reached its peak after the hottest part of the day and varied from site to site (Figures 4). While the temperature gradient at stratified sites decreased as the sun set, the water column remained generally stable, with the near-bed, mid, and near-surface layers of water retaining distinct thermal signatures (Figure 4).

    The supercritical values of Richardson number, that is, $\mathbb{R}i > 0.25$, indicate stratification at all "true" alcoves at which flow velocities were measured. This fact, and the lack of a determinative threshold in temperature gradient in the side channel led to the inference that all ponds and alcoves (except for W206.6L-Alc) were stratified, and that water in side channels was unlikely to be stratified. For cases of side channels with large cross-sectional area and sufficiently low discharge, stratification might develop. Following this inference, all column-days in all ponds and all alcoves except W206.6L-Alc were included in the calculation and assessment of the HIN index. In addition, column-days during low stage at the mouth of W208.5R-SC were also included in the HIN index calculation. Column-days recorded at the mouth of W208.5R-SC after the rise in river stage, on the other hand, were not included in $\mathbb{H}_{in}$ calculations. In total, 546 column-days logged at stratified sites.

    Note that stratification does not imply that water near the bed is cool. For some stratified column-days, such as all column-days at W206.0L-Alc, temperatures are generally warmer than in the main channel, less so near the bed: near-bed temperatures are about 0.5°C warmer than the main channel, while near-surface temperatures are close to 5.5°C warmer (Figure 4). In contrast, for other stratified column-days,

NOVEL DIMENSIONLESS INDEX FOR PHYSICALLY BASED ASSESSMENT OF
THERMAL REFUGIA CHARACTERIZES OFF-CHANNEL HABITAT ON GRAVEL BED RIVER

627

AMERICAN WATER RESOURCES ASSOCIATION

JAWRA
JOURNAL OF THE AMERICAN WATER RESOURCES ASSOCIATION
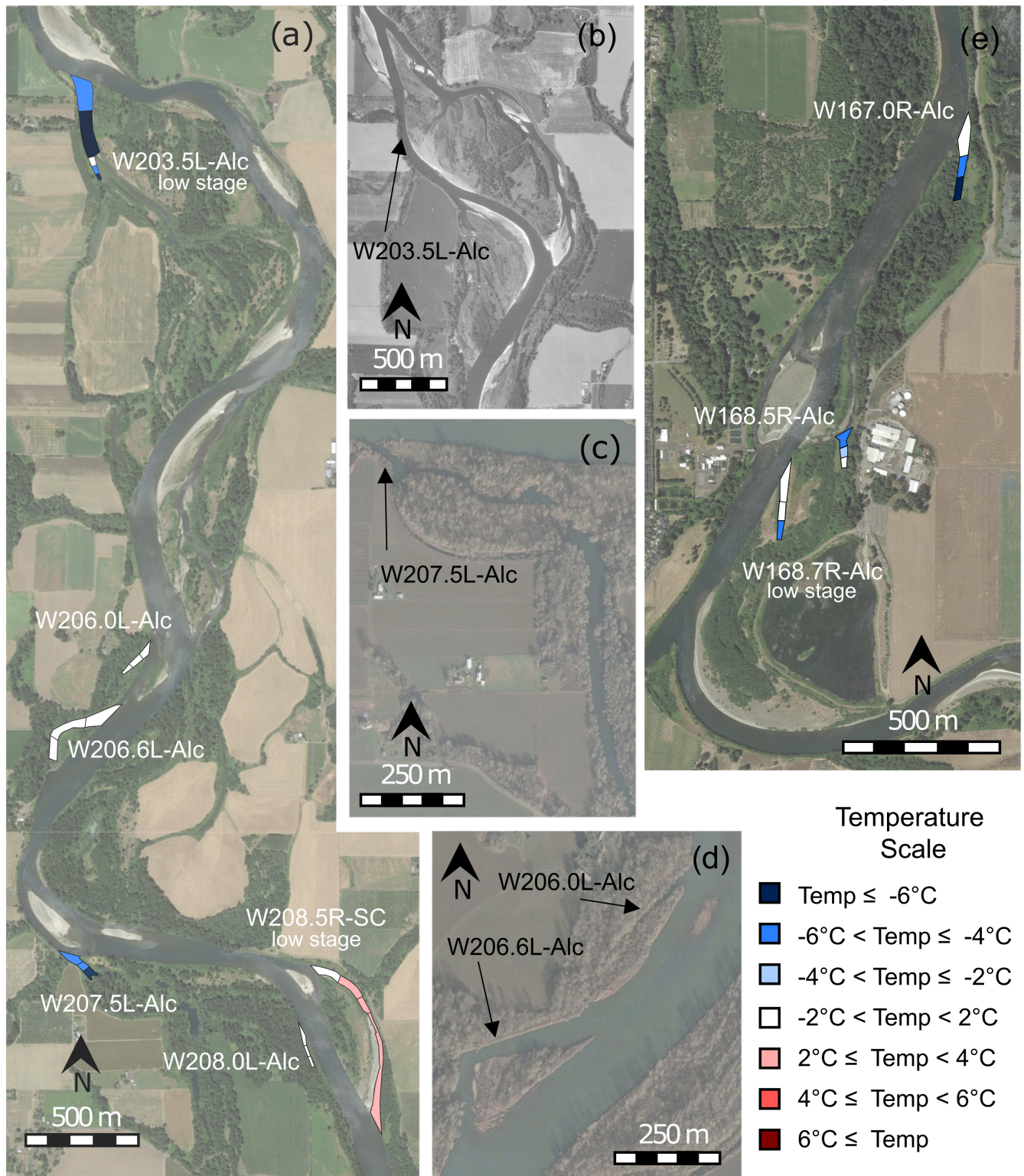
FIGURE 5 Geographic distribution of averaged near-bed bottom-station temperature measurements for all alcoves and side channel. Harrisburg reach sites appear on (a) Google earth aerial imagery from June 2017. Historical Google earth aerial imagery from May 1994 shows the main channel flowing through the current location of W203.5L-Alc (b). Google earth imagery from February 2003 shows high stage channel paths for W207.5L-Alc (c), and W206.0L-Alc (d). Corvallis reach sites appear on Google earth imagery (e) from June 2017. Temperature differences shown are in comparison to the main channel temperature at the time of the near-bed temperature measurements at secondary channel features.
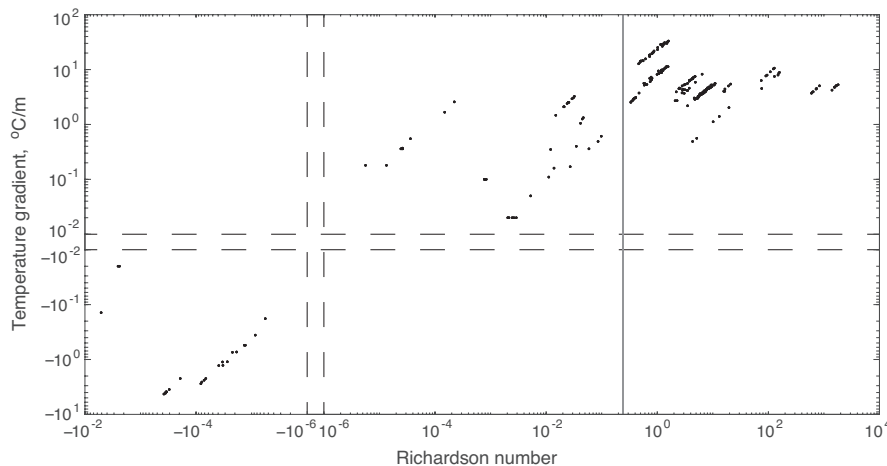
FIGURE 6 Temperature gradient versus Richardson number for each column-day at sites with applicable velocity measurements. Positive and negative values of both are shown and separated by dashed lines. Vertical gray line indicates the critical value (0.25) of Richardson number. Below this threshold, lower values indicate higher degrees of turbulence.

temperatures in the near-bed and near-surface strata straddle the temperatures in the main channel: near-bed temperatures at W207.5-Alc during low river stage are up to 7°C cooler than the mainstem, while near-surface temperatures are 3.5°C warmer than the main channel (i.e., spanning a range of 10.5°C; Figure 4).

4.3.2 | HIN index predicts measured temperatures

Temperature measurements for all stratified alcoves and ponds served to ground-truth our calculated $\mathbb{H}_{in}$ values. We expect temperatures of hyporheic inflows to alcoves, ponds, and side channels, to approach the mean annual stream temperature as subsurface residence times approach 1 year. To the extent that the HIN index captures this expectation, we expect station-days with greater $\mathbb{H}_{in}$ values to have temperatures closer to the mean annual stream temperature. Therefore, to assess the predictive power of $\mathbb{H}_{in}$ with measured temperatures, we calculated a temperature difference relative to the annual mean, $\Delta T_{sa} = T_{s,max} - T_a$, for each station-day, where $T_{s,max}$ is daily maximum temperature at a station, and T_a is the annual mean stream temperature for the Harrisburg and Corvallis reaches, specifically the mean of instantaneous temperatures recorded at 15-min intervals at the Harrisburg and Albany gages, respectively, during the 2017 calendar year (Table 2). Our use of $T_{s,max}$ rather than the mean for a station-day was motivated by ODEQ temperature thresholds (2007), which apply to the maximum temperature on a given day and in turn hold biological significance.

The $\mathbb{H}_{in}$ values calculated for all station-days (bottom, middle, and top) at stratified sites, 1638 station-days in all, appear in Figure 7. Given the large amount of scatter, value-pairs for individual station-days are binned according to $\mathbb{H}_{in}$ values so that each bin contains approximately 100 data points. Average values for each bin are also plotted in Figure 7. In general, as $\mathbb{H}_{in}$ increases, temperature difference, ΔT_{sa}, decreases. Bin-averaging markedly reduces the scatter, and the logarithmic fit to the bin-averaged values explains a large fraction of their variance (Figure 7).

Averages for each secondary channel feature site are shown only for bottom stations. At sites where data were collected both before and after the increase in stage at the beginning of August, site-days before and after the change were treated as different sites for calculation of the site averages (Table 1). Whereas bin-averaging according to the $\mathbb{H}_{in}$ markedly decreases the scatter about the trend, averaging by site has little effect. The scatter in site averages for bottom stations only is less than the scatter among all station-days, but site averages for middle and top stations are not shown in Figure 7.

5 | DISCUSSION

5.1 | Characterization of thermal regimes with dimensionless quantities

Thermal regimes of secondary channel features vary not only in time, but also in space. Measurements from the off-channel sites, that is, alcoves, ponds, and side channels, show that stratification seems to be a necessary condition for cold water areas. However, stratification alone does not guarantee that water at a site will be cool. The physically based HIN index aims to capture the dominant physical processes that do produce cold water in secondary channel features.

NOVEL DIMENSIONLESS INDEX FOR PHYSICALLY BASED ASSESSMENT OF
THERMAL REFUGIA CHARACTERIZES OFF-CHANNEL HABITAT ON GRAVEL BED RIVER

JAWRA

JOURNAL OF THE AMERICAN WATER RESOURCES ASSOCIATION

| 629
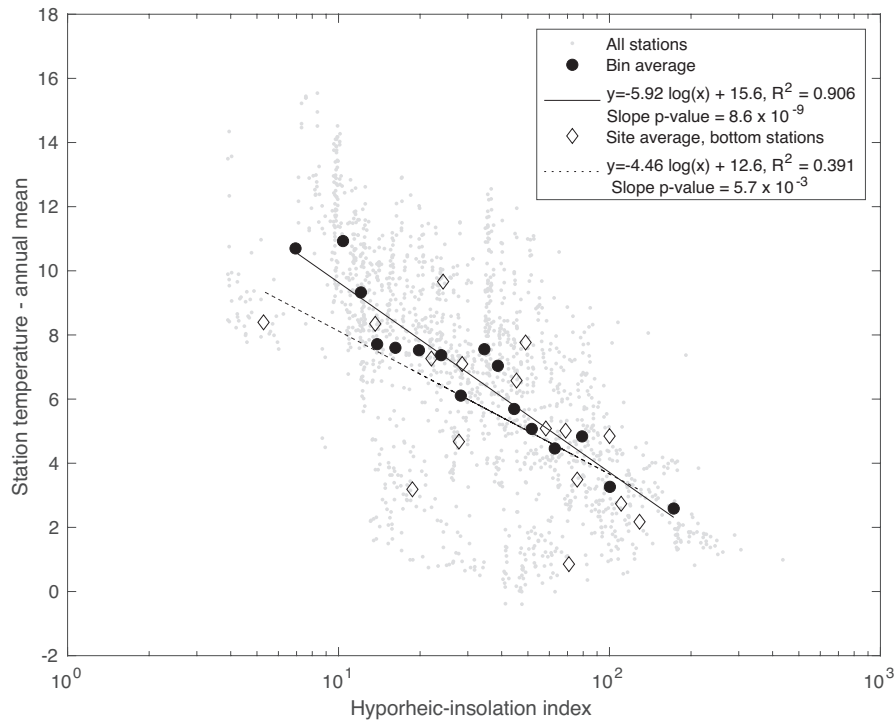
FIGURE 7 Temperature difference, ΔT_{sa}, versus hyporheic insolation index, $\mathbb{H}_{in}$, for all station-days (bottom, middle, and top) from stratified column-days, 1368 station-days in all, as well as bin-averaged (solid circles) and site-averaged (hollow diamond) values.

The HIN index predicts the presence of cool water in stratified features on average, but there is substantial scatter in the data for individual station-days. By averaging the points into bins based on $\mathbb{H}_{in}$ values alone, the fit of the logarithmic trendline, $R^2 = 0.91$, is greater than the fit of the logarithmic trendline produced by averaging $\mathbb{H}_{in}$ values by site, $R^2 = 0.39$. This discrepancy is likely the result of physical processes at an individual site that are not captured well in $\mathbb{H}_{in}$ calculations.

When grouped by site, averaged $\mathbb{H}_{in}$ values amplify quantities with significant uncertainties. These include hydraulic conductivity (K), insolation attenuation coefficient (ζ), mainstem length corresponding to the dominant hyporheic flowpath (L_{ms}), and reach-scale stream gradient (S_o). Estimates of the latter two are likely to be within a factor of two or so and are inside the square-root (3), so these are not likely to be large sources of uncertainty. The accuracy of L_{ms} and S_o could be improved through measurement with field surveys or LiDAR topography. Hydraulic conductivity and attenuation coefficient are more problematic. Hydraulic conductivity, which was estimated from previous measurements and surface vegetation, is well known for its extreme variability (Stewardson et al., 2016). While literature values for K were based on slug tests on a gravel bar on the Harrisburg Reach (Fernald et al., 2006), estimation of site age was accomplished with aerial photographs. Only having a known hydraulic conductivity value for a young site does not validate the estimated K values for "developing" and "mature" sites. Attenuation coefficient values increase with the presence of aquatic vegetation in the water column, and uncertainty in this quantity is amplified by an exponential dependence. While our field observations allowed for variation of the attenuation coefficient to reflect the presence or absence of aquatic vegetation, Secchi depth measurements were not collected. Preliminary calculations of the HIN index were all based on the same attenuation coefficient: =1/m. However, data from eutrophic lakes in Oregon include attenuation coefficient values as high as 3.4/m (Dodds & Whiles, 2010). This number reflects the presence of significant aquatic vegetation. Decreasing these uncertainties further could provide a clearer picture and an improved fit to the site averaged data. For example, determination of attenuation coefficients with depths recorded by a Secchi disk would likely reduce scatter. Even so, the logarithmic fit to bin-averaged station-day $\mathbb{H}_{in}$ points had $R^2 = 0.91$.

The HIN index is formulated to predict thermal refugia resulting from thermal buffering along long hyporheic flowpaths while ignoring thermal refugia created by lagging in shorter flowpaths. Burkholder et al. collected water temperature data on the nearby Clackamas River that suggested hyporheic lagging in larger rivers produces local variation in hyporheic discharge by only a few degrees (2008). In contrast, data collected at monitoring wells installed by Faulkner et al. (2020) on the upper Willamette just upstream of our Harrisburg reach showed hyporheic water temperatures buffered up to 7°C. On large gravel-bed rivers like the Willamette, the HIN index can capture thermal refugia produced by buffering relatively well. In smaller streams where lagging plays a more dominant role, the HIN index is unlikely to be able to completely characterize thermal refugia.

630 JAWRA
JOURNAL OF THE AMERICAN WATER RESOURCES ASSOCIATION
AMERICAN
WATER RESOURCES
ASSOCIATION

GOMBERT ET AL.

5.2 | Physical processes controlling water temperature in secondary channel features

Our data and analyses suggest that water temperature in secondary channel features on gravel-bed rivers is controlled in part by surface water. The characteristics of hyporheic discharge, which are associated with subsurface flowpath qualities, likely also play a role. Slow surface water, such as those found in most alcoves and ponds, allow the water column to reach dynamic stability and become stratified. Likewise, subsurface flowpaths that appear to be sufficiently long, have high-permeability substrates, and include preferential hydraulic gradients are likely to be associated with cool hyporheic discharge. Indeed, data from our all of our study sites show stratification is a necessary condition for the presence of cold water above the bed.

Patterns in temperature data collected at study sites coupled with physical principles suggest a hierarchy of control for heat transfer processes at the secondary channel features we instrumented. Specifically, (1) advection/dispersion, (2) insolation, and (3) subsurface inflow serve as "knobs" in the heat budget of a site that modulate its observed thermal regime. Without significant advection/dispersion, which lead to mixing throughout the water column, a stratified site produces layers of warmer, near-surface water heated by insolation and cooler, near-bed water sourced by hyporheic flow.

During our study, river stage of the main channel impacted surface water inflow into secondary channel features. This, in turn, impacted the presence of stratification of the water column (e.g., W208.5R-SC, Figure 4). A reservoir drawdown in summer 2017 caused discharge at the USGS Harrisburg Gage to almost double (i.e., 120–215 m^3/s). Increases were also recorded in discharge measurements with a flow meter in the side channel, W208.5R-SC. Measured discharge in, (1) the shallow upstream section of the side channel, and (2) the head of the deeper section of the side channel was 0.20 and 0.255 m^3/s, respectively, on July 21, prior to the drawdown; on August 9, after the drawdown commenced, measured discharge was 2.33 and 2.94 m^3/s, respectively, at the two locations. This 10× increase in discharge was accommodated in the shallow channel by both a 4× increase in the average flow velocity, from 0.13 to 0.54 m/s, as well as a 2.5× increase in cross-sectional area, from 1.63 to 4.33 m^2. In the deep section of the side channel, the average flow velocity increased from 0.0786 to 0.936 m/s and, like the shallow channel, was associated with an increase in both discharge and cross-sectional area. Figure 4 shows that the stratification that was present for the column located at the mouth of W208.5R-SC before the drawdown. It also shows the mouth's well-mixed, post-drawdown water column, which is associated with a decrease in the Richardson number from a supercritical value near 0.4 to a subcritical value near 0.004.

While the lack of similarly paired flow data from multiple study sites precludes the development of a general relationship between main channel discharge and water velocities observed in secondary channel features, it is clear that an increase in mainstem stage and the concomitant increase in discharge in side channels can effectively "flip the switch" on stratification, which is, in turn, a necessary condition for development of cool water in secondary channel features. Indeed, continuous temperature and DO measurements collected in secondary channel features on the Willamette River during summer 2016 further support this observation (Smith et al., 2020). Thus, an increase in discharge aimed at decreasing mainstem water temperature could actually eliminate some cool-water refuges. That said, we should emphasize the "could": while stratified, the bottom water at the mouth of W208.5R-SC was not cool relative to the main channel, and we did not find that any potential cool-water refuges were eliminated as a result of the August 2017 increase in stage.

Hyporheic exchange in stratified study sites was likely influenced by two types of standing water on the floodplain. First, beaver ponds have been shown to influence hydrologic processes downstream of dams during both low-flow and peak flow periods (Westbrook et al., 2006). Beaver ponds were found upstream of three of the alcoves in this study, W206.6L-Alc, W203.5L-Alc, and W168.5R-Alc, and likely influenced hyporheic exchange in these floodplain areas. Second, gravel pits, which form human-made ponds, were also adjacent to all three alcoves in the Corvallis study reach. While impacts of such human floodplain modifications on hyporheic exchange and water table levels have not been studied for the upper Willamette, it is possible gravel ponds influence the thermal regime of nearby secondary channel features.

Finally, while our study did not measure groundwater signature of water in secondary channel features, it is possible that groundwater inputs also control the thermal regimes of stratified alcoves and side channels. In the hyporheic zone, surface water, which is predominantly sourced in the High Cascades and isotopically lighter, can mix with groundwater inputs, which are predominantly sourced from alluvial fans in the valley and isotopically heavier. Past measurements by Hinkle et al. (2001) of stable isotopes in water samples from the mainstem Willamette and secondary channel features have shown that groundwater sources fed some off-channel features, at least at the time of sampling. However, isotopic analyses by Fernald et al. (2006) of samples from the river, alcoves, and shallow wells in the hyporheic zone in the Harrisburg and Corvallis reaches show that isotopic signatures cluster with the river water and appear to rule out inputs from deep groundwater. Additional testing of water samples from study sites could provide additional evidence for the role groundwater plays in shaping the thermal regime of secondary channel features. Even so, whereas groundwater sources may produce cool water in some secondary features, such sources are not necessary to explain the cool water we found, nor do groundwater sources seem particularly likely at any of our sites.

5.3 | Relationship between thermal regimes and habitat quality

Water temperature is one of the defining habitat characteristics for anadromous cold water fishes. Temperature standards of the Oregon Department of Environmental Quality categorize areas that are at least 2°C cooler than the mainstem during the time of the mainstem daily maximum as cold water refugia for salmonids. Out of our seven stratified alcoves, five have at least one location with water temperature measurements that are at least 2°C cooler than the mainstem at the time of the daily maximum temperature: W207.5L-Alc, W203.5L-Alc, W168.7R-Alc, W168.5R-Alc, and W167R-Alc. However, legally defined cold water refuges do not necessarily provide all ecosystem services required by cold water fishes. In particular, the ODEQ standard defines an area that is cooler relative to the mainstem as a thermal refuge, even if the temperature of the secondary channel feature still exceeds physiological limits for cold water fishes.

Biologically relevant cold water refuges provide not only cold water but also sufficient DO. Two of the stratified sites cooler than the main channel, W207.5L-Alc and W203.5L-Alc, provide at least 6.0 mg/L at near-bed depths. However, the cool areas of W168.7R-Alc and W168.5R-Alc provide <2 mg/L of DO just above the bed. While these two alcoves meet the legal definition of a cold water refuge, the ecosystem services they provide may not be biologically sufficient for salmonids. While DO point measurements were not taken at W167R-Alc, the density of macrophytes may actually suggest the presence of hypoxic conditions. If the observed aquatic vegetation includes *Ludwigia hexapetala*, DO levels may be below 6.0 mg/L. Because Ludwigia is an emergent aquatic plant, its leaves exchange gases with the atmosphere rather than the water column (Rose & Crumpton, 1996). Atmospheric exchange results in depleted levels of DO in the water itself. Thus, while secondary channel features with *L. hexapetala* may meet the legal definition of a cold water refuge, these sites may be too DO-impaired to provide suitable habitat for salmonids.

Hyporheic exchange affects both the temperature and the DO concentration of water flowing through the subsurface. DO levels of hyporheic water are lower than those of river water (Fernald et al., 2006). As a result, hyporheic discharge in secondary channel features is often hypoxic. Residence times longer than 6.9 h are associated with net hypoxic conditions and anaerobic microbial processes (Zarnetske et al., 2011). While hyporheic discharge may be cool, it may not provide suitable habitat for cold water fishes. In our study, the two stratified alcoves that are DO-impaired, W168.7R-Alc and W168.5R-Alc, have the lowest DO readings at the locations with the coolest temperatures. Both of these water quality parameters may be the result of long subsurface flowpaths and long residence times in the hyporheic zone. However, it is important to note that the DO readings captured by point measurements taken may not be representative of the entire site; DO varies in time and space on secondary features in the Willamette River (Smith et al., 2020). It is possible that, during another time of day, especially during the afternoon when DO levels peak, these sites may be less DO-impaired. Furthermore, it is possible for some species of fish to continue to survive in DO-impaired habitat, even if their growth is stunted (Zinn et al., 2021).

DO values in this study are based on point measurements. Often, a single measurement was taken at each column and at each station for each site. While attempts were made to position the instrument at a location that corresponded to a station at a given column before readings were recorded, there was likely measurement error. For example, some near-bed measurements may have recorded values taken while the DO probe was submerged in bed sediment, resulting in especially low readings. Deploying a DO probe to record continuous measurements at known station elevations in the water column would provide more robust data to inform habitat quality assessments.

5.4 | Restoration implications

The ability to identify potential cold water areas in large gravel-bed rivers holds implications for successful restoration of ecosystem services in modified basins. Required inputs for the HIN index can be obtained from (a) aerial photographs, (b) stream gages, (c) meteorological stations, (d) literature values, and (e) water depth measurements. The values used to calculate $\mathbb{H}_{in}$ for this study were based on aerial images from Google Earth, water temperature data collected in the main channel at USGS gages 14166000 (Willamette River, Harrisburg, OR) and 14174000 (Willamette River, Albany, OR), daily solar radiation data from USBR AgriMet Weather Station (Corvallis, Oregon), published values of slope and hydraulic conductivity for the upper Willamette (Dykaar & Wigington, 2000; Fernald et al., 2006), and values for attenuation coefficient of lakes in Oregon (Dodds & Whiles, 2010). The only field measurements required were the depths of secondary channel features.

6 | CONCLUSIONS

Rivers such as the Willamette have mainstem temperatures too warm for cold water fishes during periods of rearing and migration. However, the likelihood of addressing this challenge by significantly cooling the main channel is small. Instead, we are working to advance our understanding of processes controlling thermal regimes of secondary channel features along gravel-bed rivers. With the predictive physically based HIN index, the thermal regimes of secondary channel features may be characterized based on heat-exchange process. With minimal field data,

the HIN index can predict which off channel features may provide thermal refugia resulting from thermal buffering along sufficiently long hyporheic flowpaths.

Secondary channel features that provide thermal refuges to cold water fishes on the upper Willamette River are characterized by stratification. Surface water inflow, which leads to mixing throughout the water column, precludes the development of layers of cooler near-bed water sourced by hyporheic flow that are situated beneath warmer, near-surface water heated by insolation. In this study, the side channel and alcove with significant surface water inflow were well-mixed and were not cooler than the mainstem. Furthermore, alcoves and ponds that were warmer than the mainstem, while stratified, appeared to have hyporheic flowpaths that were either short in length or had low hydraulic conductivity, or both. Even at sites cooler than the mainstem, DO measurements indicate some cold water may be too hypoxic for fish. Ultimately, both temperature and fish use data are needed to paint a complete picture of habitat quality in secondary channel features. Even so, this study sheds light on the physical processes that govern water temperature in secondary channel features on gravel-bed rivers, moving efforts to identify and preserve thermal refugia in a more quantifiable direction.

AUTHOR CONTRIBUTIONS

Carolyn E. Gombert: Data curation, formal analysis, funding acquisition, investigation, methodology, resources, visualization, writing – original draft, writing – review and editing. **Stephen T. Lancaster:** Conceptualization; formal analysis; funding acquisition; investigation; methodology; resources; supervision; writing – review and editing. **Gordon E. Grant:** Formal analysis; funding acquisition; investigation; methodology; supervision; writing – review and editing. **Rebecca L. Flitcroft:** Funding acquisition; Investigation; methodology; resources; supervision; writing – review and editing.

CONFLICT OF INTEREST

All authors declare that they have no conflicts of interest.

DATA AVAILABILITY STATEMENT

The data that support the findings of this study are openly available in the Consortium of Universities for the Advancement of Hydrologic Science at https://doi.org/10.4211/his-5671.

ORCID

Carolyn E. Gombert https://orcid.org/0000-0002-5198-6303

REFERENCES

Arrigoni, A.S., G.C. Poole, L.A.K. Mertes, S.J. O'Daniel, W.W. Woessner, and S.A. Thomas. 2008. "Buffered, Lagged, or Cooled? Disentangling Hyporheic Influences on Temperature Cycles in Stream Channels." *Water Resources Research* 44(9): 1–13. https://doi.org/10.1029/2007WR006480.

Arscott, D.B., K. Tockner, and J.V. Ward. 2001. "Thermal Heterogeneity along a Braided Floodplain River (Tagliamento River, Northeastern Italy)." *Canadian Journal of Fisheries and Aquatic Sciences* 58(12): 2359–73. https://doi.org/10.1139/cjfas-58-12-2359.

Beschta, R.L., and R.L. Taylor. 1988. "Stream Temperature Increases and Land Use in a Forested Oregon Watershed." *Water Resources Bulletin* 24: 19–25. https://doi.org/10.1111/j.1752-1688.1988.tb00875.x.

Burkholder, B.K., G.E. Grant, R. Haggerty, T. Khangaonkar, and P.J. Wampler. 2008. "Influence of Hyporheic Flow and Geomorphology on Temperature of a Large, Gravel-Bed River, Clackamas River, Oregon, USA." *Hydrological Processes* 22: 941–53. https://doi.org/10.1002/hyp.6984.

Caissie, D. 2006. "The Thermal Regime of Rivers: A Review." *Freshwater Biology* 51(8): 1389–406. https://doi.org/10.1111/j.1365-2427.2006.01597.x.

Cole, T.M., and S.A. Wells. 2006. *CE-QUAL-W2: A Two-Dimensional, Laterally Averaged, Hydrodynamic and Water Quality Model, Version 3.5 (Instruction Report EL-06-1).* Vicksburg, MS: U.S. Army Engineering and Research Development Center.

Dodds, W.K., and M.R. Whiles. 2010. *Freshwater Ecology: Concepts and Environmental Applications.* Burlington, MA: Academic Press.

Dugdale, S.J., R.A. Curry, A. St-Hilaire, and S.A. Andrews. 2018. "Impact of Future Climate Change on Water Temperature and Thermal Habitat for Keystone Fishes in the Lower Saint John River, Canada." *Water Resources Management* 32: 4853–78. https://doi.org/10.1007/s11269-018-2057-7.

Dugdale, S.J., D.M. Hannah, and I.A. Malcolm. 2017. "River Temperature Modelling: A Review of Process-Based Approaches and Future Directions." *Earth-Science Reviews* 175: 97–113. https://doi.org/10.1016/j.earscirev.2017.10.009.

Dykaar, B.B., and P.J. Wigington. 2000. "Floodplain Formation and Cottonwood Colonization Patterns on the Willamette River, Oregon, USA." *Environmental Management* 25(1): 87–104. https://doi.org/10.1007/s002679910007.

NOVEL DIMENSIONLESS INDEX FOR PHYSICALLY BASED ASSESSMENT OF
THERMAL REFUGIA CHARACTERIZES OFF-CHANNEL HABITAT ON GRAVEL BED RIVER

633

Dzara, J.R., B.T. Neilson, and S.E. Null. 2019. "Quantifying Thermal Refugia Connectivity by Combining Temperature Modeling, Distributed Temperature Sensing, and Thermal Infrared Imaging." *Hydrology and Earth System Sciences* 23: 2965–82. https://doi.org/10.5194/hess-23-2965-2019.

Ebersole, J.L., W.J. Liss, and C.A. Frissell. 2001. "Relationship between Stream Temperature, Thermal Refugia and Rainbow Trout *Oncorhynchus mykiss* Abundance in Arid-Land Streams in the Northwestern United States." *Ecology of Freshwater Fish* 10(1): 1–10. https://doi.org/10.1034/j.1600-0633.2001.100101.x.

Ebersole, J.L., W.J. Liss, and C.A. Frissell. 2003. "Thermal Heterogeneity, Stream Channel Morphology, and Salmonid Abundance in Northeastern Oregon Streams." *Canadian Journal of Fisheries and Aquatic Sciences* 60(10): 1266–80. https://doi.org/10.1139/f03-107.

Faulkner, B.R., J.R. Brooks, D.M. Keenan, and K.J. Forshay. 2020. "Temperature Decrease along Hyporheic Pathlines in a Large River Riparian Zone." *Ecohydrology* 13: e2160. https://doi.org/10.1002/eco.2160.

Fernald, A.G., D.H. Landers, and P.J. Wigington. 2006. "Water Quality Changes in Hyporheic Flow Paths between a Large Gravel Bed River and Off-Channel Alcoves in Oregon, USA." *River Research and Applications* 22(10): 1681–794. https://doi.org/10.1002/rra.961.

Fullerton, A.H., C.E. Torgersen, J.J. Lawler, E.A. Steel, J.L. Ebersole, and S.Y. Lee. 2018. "Longitudinal Thermal Heterogeneity in Rivers and Refugia for Coldwater Species: Effects of Scale and Climate Change." *Aquatic Sciences* 80(1): 3–15. https://doi.org/10.1007/s00027-017-0557-9.

Gleick, P.H. 2000. "A Look at Twenty-First Century Water Resources Development." *Water International* 25(1): 127–38. https://doi.org/10.1080/02508060008686804.

Gombert, C.E., S.T. Lancaster, R.L. Flitcroft, and G.E. Grant. 2020. "Water Temperature of Secondary Channel Features in Upper Willamette River, Oregon, USA." CUAHSI Data Release. https://doi.org/10.4211/his-5671.

Hannah, D.M., and G. Garner. 2015. "River Water Temperature in the United Kingdom: Changes over the 20th Century and Possible Changes over the 21st Century." *Progress in Physical Geography: Earth and Environment* 39(1): 68–92. https://doi.org/10.1177/0309133314550669.

Hinkle, S.R., J.H. Duff, F.J. Triska, A. Laenen, E.B. Gates, K.E. Bencala, D.A. Wentz, and S.R. Silva. 2001. "Linking Hyporheic Flow and Nitrogen Cycling Near the Willamette River—A Large River in Oregon, USA." *Journal of Hydrology* 244(3–4): 157–80. https://doi.org/10.1016/S0022-1694(01)00335-3.

Hulse, D., S.V. Gregory, and J. Baker. 2002. *Willamette River Basin Planning Atlas: Trajectories of Environmental and Ecological Change.* Corvallis, OR: Oregon University Press.

Jackson, F.L., D.M. Hannah, V. Ouellet, and I.A. Malcom. 2021. "A Deterministic River Temperature Model to Prioritize Management of Riparian Woodlands to Reduce Summer Maximum River Temperatures." *Hydrological Processes.* 35(8). https://doi.org/10.1002/hyp.14314.

Johnson, S.L. 2004. "Factors Influencing Stream Temperatures in Small Streams: Substrate Effects and a Shading Experiment." *Canadian Journal of Fisheries and Aquatic Sciences* 61(6): 913–23. https://doi.org/10.1139/f04-040.

Johnson, S.L., and J.A. Jones. 2000. "Stream Temperature Responses to Forest Harvest and Debris Flows in Western Cascades, Oregon." *Canadian Journal of Fisheries and Aquatic Sciences* 57(S2): 30–39. https://doi.org/10.1139/f00-109.

Lancaster, S.T., and R. Haggarty. 2012. "Assessing the Effects of Restoration of the Marsing Reach of the Middle Snake River: Comprehensive Linked Programs of Modeling and Monitoring." Proposal Prepared for the Freshwater Trust (Unpublished).

O'Connor, J.E. 2001. "Origin, Extent, and Thickness of Quaternary Geologic Units in the Willamette Valley, Oregon (Professional Paper No. 1620)." U.S. Geological Survey. https://pubs.usgs.gov/pp/1620/pdf/pp1620.pdf.

ODEQ. 2007. "340-041-0028: Water Quality Standards: Beneficial Uses, Policies, and Criteria for Oregon—Temperature." Oregon Department of Environmental Quality. https://secure.sos.state.or.us/oard/viewSingleRule.action?ruleVrsnRsn=244176.

Peixoto, J.P., and A.H. Oort. 1992. *Physics of Climate.* New York: American Institute of Physics.

Poole, G.C., and C.H. Berman. 2001. "An Ecological Perspective on In-Stream Temperature: Natural Heat Dynamics and Mechanisms Of Human-Caused Thermal Degradation." *Environmental Management* 27(6): 787–802. https://doi.org/10.1007/s002670010188.

Rose, C., and W.G. Crumpton. 1996. "Effects of Emergent Macrophytes on Dissolved Oxygen Dynamics in a Prairie Pothole Wetland." *Wetlands* 16(4): 495–502. https://doi.org/10.1007/BF03161339.

Rounds, S.A., and L.E. Stratton Garvin. 2022. "Tracking Heat in the Willamette River system, Oregon." U.S. Geological Survey Scientific Investigations Report 2022–5006, 47 pp. https://doi.org/10.3133/sir20225006.

Rumble, J.R., ed. 2018. "CRC Handbook of Chemistry and Physics (99th Edition)." CRC Press. http://hbcponline.com.

Schroeder, R.K., L.D. Whitman, B. Cannon, and P. Olmsted. 2016. "Juvenile Life-History Diversity and Population Stability of Spring Chinook Salmon in the Willamette River Basin, Oregon." *Canadian Journal of Fisheries and Aquatic Sciences* 73(6): 921–34. https://doi.org/10.1139/cjfas-2015-0314.

Sedell, J.R., G.H. Reeves, F.R. Hauer, J.A. Stanford, and C.P. Hawkins. 1990. "Role of Refugia in Recovery from Disturbances: Modern Fragmented and Disconnected River Systems." *Environmental Management* 14: 711–24. https://doi.org/10.1007/BF02394720.

Shaftel, R., S. Mauger, J. Falke, D. Rinella, J. Davis, and L. Jones. 2020. "Thermal Diversity of Salmon Streams in the Matanuska-Susitna Basin, Alaska." *Journal of the American Water Resources Association* 56: 630–46. https://doi.org/10.1111/1752-1688.12839.

Smith, C.D., J.F. Mangano, and S.A. Rounds. 2020. "Temperature and Water-Quality Diversity and the Effects of Surface-Water Connection in Off-Channel Features of the Willamette River, Oregon, 2015–16." U.S. Geological Survey Scientific Investigations Report 2020-5068, 70 pp. https://doi.org/10.3133/sir20205068.

Stevens, B.S., and J.M. DuPont. 2011. "Summer Use of Side-Channel Thermal Refugia by Salmonids in the North Fork Coeur d'Alene River, Idaho." *North American Journal of Fisheries Management* 31(4): 683–92. https://doi.org/10.1080/02755947.2011.611037.

Stewardson, M.J., T. Datry, N. Lamouroux, H. Pella, N. Thommeret, L. Valette, and S.B. Grant. 2016. "Variation in Reach-Scale Hydraulic Conductivity of Streambeds." *Geomorphology* 259: 70–80. https://doi.org/10.1016/j.geomorph.2016.02.001.

Tonolla, D., V. Acuña, U. Uehlinger, T. Frank, and K. Tockner. 2010. "Thermal Heterogeneity in River Floodplains." *Ecosystems* 13: 727–40. https://doi.org/10.1007/s10021-010-9350-5.

Torgersen, C.E., D.M. Price, H.W. Li, and B.A. McIntosh. 1999. "Multiscale Thermal Refugia and Stream Habitat Associations of Chinook Salmon in Northeastern Oregon." *Ecological Applications* 9(1): 301–19. https://doi.org/10.1890/1051-0761(1999)009[0301:MTRASH]2.0.CO;2.

van Vliet, M.T., W.H.P. Franssen, J.R. Yearsley, F. Ludwig, I. Haddeland, D.P. Lettenmaier, and P. Kabat. 2013. "Global River Discharge and Water Temperature under Climate Change." *Global Environmental Change* 23(2): 450–64. https://doi.org/10.1016/j.gloenvcha.2012.11.002.

Wallick, J.R., G.E. Grant, S.T. Lancaster, J.P. Bolte, and R.P. Denlinger. 2007. "Patterns and Controls on Historical Channel Change in the Willamette River, Oregon, USA." In *Large Rivers: Geomorphology and Management*, edited by A. Gupta, 491–516. West Sussex, UK: John Wiley & Sons.

Wallick, J. R., K.L. Jones, J.E. O'Connor, M.K. Keith, D. Hulse, and S.V. Gregory. 2013. "Geomorphic and Vegetation Processes of the Willamette River floodplain, Oregon-Current Understanding and Unanswered Questions (Open File Report 2013-1246)." U.S. Geological Survey. https://doi.org/10.3133/ofr20131246.

Wallick, J.R., S.T. Lancaster, and J.P. Bolte. 2006. "Determination of Bank Erodibility for Natural and Anthropogenic Bank Materials Using a Model of Lateral Migration and Observed Erosion along the Willamette River, Oregon, USA." *River Research and Applications* 22(6): 631–49. https://doi.org/10.1002/rra.925.

Westbrook, C.J., D.J. Cooper, and B.W. Baker. 2006. "Beaver Dams and Overbank Floods Influence Groundwater–Surface Water Interactions of a Rocky Mountain Riparian Area." *Water Resources Research* 42(6). https://doi.org/10.1029/2005WR004560.

Zarnetske, J.P., R. Haggerty, S.M. Wondzell, and M.A. Baker. 2011. "Dynamics of Nitrate Production and Removal as a Function of Residence Time in the Hyporheic Zone." *Journal of Geophysical Research: Biogeosciences* 116(G1). https://doi.org/10.1029/2010JG001356.

Zinn, K. R., Jordan S. Rosenfeld, and Eric B. Taylor. 2021. "Effects of Experimental Flow Manipulations on Water Quality, Hypoxia, and Growth of Threatened Salish Sucker (*Catostomus* sp. cf. *catostomus*) and Juvenile Coho Salmon (*Oncorhynchus kisutch*)." *Canadian Journal of Fisheries and Aquatic Sciences* 78(9): 1234–46. https://doi.org/10.1139/cjfas-2020-01.

SUPPORTING INFORMATION

Additional supporting information can be found online in the Supporting Information section at the end of this article.

How to cite this article: Gombert, Carolyn E., Stephen T. Lancaster, Gordon E. Grant and Rebecca L. Flitcroft. 2023. "Novel dimensionless index for physically based assessment of thermal refugia characterizes off-channel habitat on gravel bed river." *Journal of the American Water Resources Association* 59(4): 615–634. https://doi.org/10.1111/1752-1688.13096.